

# Modelling and Control of Variable Stiffness Actuated Robots

Sabira Jamaludheen<sup>1</sup>, Roshin R<sup>2</sup>

P.G. Student, Department of Electrical and Electronics Engineering, MES College of Engineering, Kuttippuram, Kerala, India<sup>1</sup>

Assistant Professor, Department of Electrical and Electronics Engineering, MES College of Engineering, Kuttippuram, Kerala, India<sup>2</sup>

**ABSTRACT:** Variable Stiffness Actuation (VSA) is a recently emerged concept in Robotics with wide range of applications and advantages, especially in areas involving a high degree of Human-Robot Interaction (HRI). Variable Stiffness Actuators are a particular class of actuators with the capability of changing the apparent actuator output stiffness independently from the apparent output position. Control of VSA robots is challenging due to the intrinsic nonlinearity of their dynamics.

The system considered here is a two link manipulator with antagonistic VSA configuration. The equation of motion of the manipulator is modeled using Lagrange-Euler formulation and the model obtained is validated in MATLAB software. The objective is to achieve the tracking of a suitable trajectory assigned to the manipulator end-effector using different control strategies and to find out the best one. The response of considered system analyzed by placing PD and PID controllers in the forward path using a unit step signal as the reference. Simulation result showed that PID controller has the advantage of fast settling time and better tracking response compared to PD controller.

**KEYWORDS:** Variable Stiffness Actuation, Antagonistic Configuration, VSA Robot Manipulator, PID controller

## I. INTRODUCTION

Robotics is a branch of electrical, electronics, mechanical and computer science engineering which deals with the design, construction, operations and applications of robots. A Robot is a multi-functional reprogrammable device designed to do various tasks like pick and place, moving tools etc. Robots are generally used in factories and industries, but nowadays they tend to be found in the most technologically advanced societies such as search and rescue, military battle, mine and bomb detection and hospital care. These new domains of applications imply a closer interaction with the user. i.e, robots and humans share the workspace and also share the goals.

The potential of achieving human level performance inspired researchers to design anthropomorphic robots [1]. After initial attempts focusing on the kinematic configuration of the robots, the research focused on their dynamic behaviour in situations such as collisions, interaction with humans, objects and the environment. One approach is the design of light-weight robots with integrated torque sensors and active torque control [2]. Variable stiffness actuated (VSA) robots [3]-[7] have recently emerged in order to cope with the challenges faced by the actively torque-controlled light-weight robots. VSA robots are usually intrinsically compliant, and elastic elements in the joints are employed to store energy[8]. In this way, the robots can decrease energy consumption in repetitive tasks [9], increase maximum force and velocity capabilities, and easily absorb impacts. Moreover, the variable stiffness behaviour of the robot can protect both the robot joints and the human.

A particular aspect of variable stiffness actuators is that the stiffness variation mechanism adds an additional degree of freedom (dof) to the joint and therefore increases system complexity. This also results in increased control complexity. Regarding joint control, the literature mostly deals with independent position and stiffness control by adjusting the position or the torque of the two joint motors [10]. As high energy efficiency is desired, most of the joints developed show very low intrinsic damping. This is advantageous for tasks such as running or throwing. However, many applications need damped robot behaviour. Adding an additional variable damping element would further increase mechanism complexity and size. Therefore the damping of the VS joints is aimed to be realized by the control system.

Major control challenges are the nonlinear elasticity and the multi-input multi-output (MIMO) system properties due to the coupled arm dynamics [11].

Significant research has been carried out on the control of the VSAs. Earlier strategy proposed in literature consisted in a PD-based controller designed on the linearized actuation plant [12]. Following this, nonlinear control techniques were explored such as the feedback linearization. This strategy, mostly implemented for flexible joints, was extended to control the VSAs in [13] as well as in [14]. However, a control strategy with fixed gains may result limited in performance when the dynamic variations of the VSA become significant. Alternative approach is the gain scheduling, which adjusts the controller action on the basis of a parameter that significantly affects the linearized dynamic variations of the system. This method was implemented in [15], to control the linearized dynamics of the VSA. In contrast with the feedback linearization, this strategy uses the physical variables in the plant model, without introducing coordinate transformations.

This paper focuses on the modelling of variable stiffness actuated robots and has done a comparative study on the performance of a two link VSA manipulator with some linear control methods like PD and PID controllers. The paper is organized as follows: section II introduces the system considered for the comparative study. Section III defines the problem and section IV briefly recalls the main concepts related to the modelling of VSA robots. Controller design and simulation results are included in section V & VI respectively, while conclusions are drawn in section VII.

## II. SYSTEM DESCRIPTION

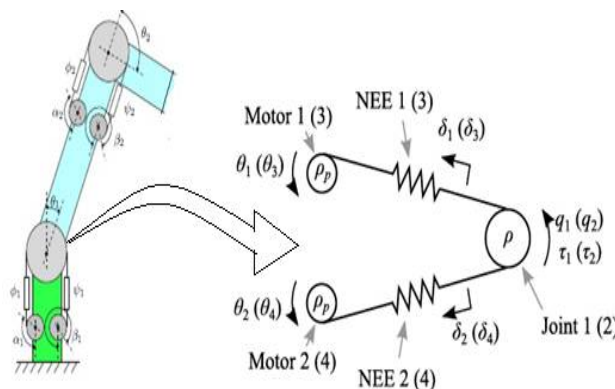


Fig.1. A two link VSA robot manipulator

The considered robot is a two-link planar manipulator (Fig.1), actuated by four servomotors connected to an equal number of nonlinear elastic elements (NEEs). Antagonistic configuration of the NEEs is considered for each of the two joints in order to achieve variable-stiffness behaviour: therefore, each joint has two NEEs Antagonistic configuration and nonlinear behaviour of the NEEs ensure variable compliance actuation. Notations used in Fig.1 are listed in Table 1.

Table 1 : Different parameters of the considered system

PARAMETER	DESCRIPTION
$q_i, i = 1,2$	Joint angles
$\theta_i, i = 1,2,3,4$	Motor angles
$\delta_i, i = 1,2,3,4$	Tendon displacements
$\rho$	Radius of joints
$\rho_p$	Radius of pulley of motor
$\tau_i, i=1,2$	Torque of joints

### III. PROBLEM DEFINITION

The variable stiffness actuation technology promises several advantages. A main difficulty of the control of the impedance parameters of VSA robots is the dynamics introduced by the separation of motor and link side and the nonlinear elasticity. Other challenges imposed by VSA robots are the multi-dimensionality of the robot system, the nonlinear robot dynamics, and the nonlinear VSA characteristics which shows low intrinsic damping. The problem considered here is achieving a faithful tracking of a suitable reference trajectory assigned to the manipulator end-effector while maintaining a desired level of active stiffness.

### IV. SYSTEM MODELLING

Optimal performance can be obtained from a robotic manipulator if sophisticated control strategies are employed. However precise control of high-speed motion requires the use of a realistic dynamic model of the arm.

The actual dynamic model of a robot manipulator can be obtained from known physical laws such as the laws of Newtonian mechanism and Lagrangean mechanism. Thus basically two modelling approaches are available.

- 1) Lagrange-Euler formulation
- 2) Newton-Euler formulation

At first the Lagrangean formulation was adopted. Complex dynamics systems can be modelled in a relatively simple, elegant fashion using Lagrange-Euler approach. It is based on the notion of generalized coordinates, energy and generalized forces. For an n-axis robotic arm, an appropriate set of generalized coordinates is the vector of n joint variables  $q$ . The components of  $q$  represent the joint angles of revolute joints and the joint distances of prismatic joints. Next an alternative approach, called the Recursive Newton-Euler formulation is developed. This approach has the advantage that it is very amenable to computer implementation and furthermore it is computationally more efficient than the Lagrangean approach. However the resulting equation of motion in Lagrange-Euler method is in a simple, easily understandable form and is suitable for examining the effects of various parameters on the motion of the manipulator. For this reason, Lagrange-Euler modelling is used in this work.

#### A. Modelling of VSA Robot

In order to model VSA robots, two sets of coordinates have to be considered. A first set  $q \in R^m$ , represents the joint angle of the robot, like in standard rigid manipulators. In addition to that, another set of coordinates  $\theta \in R^m$  accounts for the motor angles of the compliant actuators, reflected through gear reduction. Vectors  $q$  and  $\theta$  are referred to as the *link-side* and *motor-side* coordinates, respectively.

#### B. Link Side Dynamics (Lagrange- Euler Formulation)

The Lagrangean is defined as the difference between the kinetic energy and potential energy. Let  $K$  and  $V$  represent the kinetic and potential energies of the considered manipulator respectively. Then Lagrangean function  $L$  can be written as

$$L(q, \dot{q}) = K(q, \dot{q}) - V(q) \quad (1)$$

where  $\dot{q} = \frac{dq}{dt}$  is the vector of joint velocities. Note that the kinetic energy  $K$  depends on both the position and the velocity of the manipulator, while the potential energy  $V$  depends on only the joint position.

The general equation of motion of a robotic system can be formulated in terms of Lagrangean function as follows.

$$\frac{d}{dt} \left( \frac{\partial L}{\partial \dot{q}_i} \right) - \frac{\partial L}{\partial q_i} = F_i; i=1,2,\dots,n \quad (2)$$

where  $q_i$  is the coordinates by which the energies are expressed and  $F_i$  is the corresponding generalized non-potential force that drives  $q_i$ . Here  $n$  is the number of independent generalized coordinates. The Lagrangean formulation of

robot arm manipulator dynamics consists of a system of n second order non-linear differential equations in the vector of joint variables q. To specify these equations in more detail, we must formulate expressions for the kinetic energy (K), potential energy (V) and the generalized force (F).

### B1. Kinetic Energy (K)

The most complicated term in the Lagrangean function of a robotic arm is the kinetic energy of the links  $K(q, \dot{q})$ . To obtain an expression for the total kinetic energy, we begin by examining the kinetic energy of the  $i^{th}$  link. The  $i^{th}$  link will be moving in the 3 dimensional spaces with both a linear velocity and an angular velocity. Let  ${}^0v_i$  denote the linear velocity of the centre of mass of link i with respect to the robot base frame, and let  ${}^0\omega_i$  denote the angular velocity about centre of mass with respect to the base frame. Then the kinetic energy of link i may be written as

$$K_i = \frac{1}{2} ({}^0v_i)^T m_i ({}^0v_i) + \frac{1}{2} ({}^0\omega_i)^T {}^0I_i ({}^0\omega_i) \quad (3)$$

where the parameter  $m_i$  represents the mass of  $i^{th}$  link.

The translational and angular velocity vectors can be expressed based on the joint coordinate velocities, utilizing the Jacobian of link  $J_i$ .

$$\begin{bmatrix} {}^0v_i \\ {}^0\omega_i \end{bmatrix} = \begin{bmatrix} J_{vi} \\ J_{wi} \end{bmatrix} \dot{q}_i = J_i \dot{q}_i \quad (4)$$

The kinetic energy of the whole robot is then

$$\begin{aligned} K &= \sum_{k=1}^n K_k \\ &= \frac{1}{2} \sum_{k=1}^n (J_{vk} \dot{q}_k)^T m_k (J_{vk} \dot{q}_k) + (J_{wk} \dot{q}_k)^T {}^0I_k (J_{wk} \dot{q}_k) \\ &= \frac{1}{2} \dot{q}_k^T D \dot{q}_k \end{aligned} \quad (5)$$

where D is an nxn matrix called the manipulator inertia matrix and is given by

$$D = \left\{ \sum_{k=1}^n (J_{vk})^T m_k (J_{vk}) + (J_{wk})^T {}^0I_k (J_{wk}) \right\} \quad (6)$$

### B2. Potential Energy (V)

As done for kinetic energy, the total potential energy stored in the robot is given by the sum of the contributions of each link. On the assumption of rigid links, the potential energy stored in link i is defined as the amount of work required to raise the centre of mass of link i from a horizontal reference plane to its present position under the influence of gravity.

With reference to the base frame, the work required to displace link i to position  ${}^0r_i$  is given by

$$V_i = -m_i {}^0g^T {}^0r_i \quad (7)$$

Where g is the vector due to acceleration and  ${}^0r_i$  is the position vector. Hence the total potential energy stored in a robot arm is given by

$$\begin{aligned} V &= \sum_{i=1}^n V_i \\ &= \sum_{i=1}^n -m_i {}^0g^T {}^0r_i \end{aligned} \quad (8)$$

### B3. Lagrange – Euler Equations of Motion

Having computed the total kinetic and potential energies of the n- link robot manipulator at hand the equations (5) &(8) respectively, the Lagrangian of eq.(1) can be written as

$$\begin{aligned} L &= K - V \\ &= \frac{1}{2} \sum_{i=1}^n \sum_{j=1}^n D_{ij} \dot{q}_i \dot{q}_j + \sum_{i=1}^n m_i {}^0g^T {}^0r_i \end{aligned} \quad (9)$$

Next, the Lagrange function is differentiated w.r.t to  $q_i, \dot{q}_i$  and  $t$  to formulate the dynamical equation of motion. Since the potential energy does not depend on  $\dot{q}_i$ , taking the partial derivative of  $L$  given by eq.(9) w.r.t  $\dot{q}_i$  yields

$$\frac{\partial L}{\partial \dot{q}_i} = \frac{\partial (K-V)}{\partial \dot{q}_i} = \frac{\partial K}{\partial \dot{q}_i} = \sum_{j=1}^n D_{ij} \dot{q}_j ; i=1, \dots, n \quad (10)$$

Now eq.(10) is differentiated w.r.t time  $t$  as

$$\begin{aligned} \frac{d}{dt} \left( \frac{\partial L}{\partial \dot{q}_i} \right) &= \frac{d}{dt} \left( \sum_{j=1}^n D_{ij} \dot{q}_j \right) \\ &= \sum_{j=1}^n D_{ij} \ddot{q}_j + \sum_{j=1}^n \sum_{k=1}^n \frac{\partial D_{ij}}{\partial q_k} \dot{q}_k \dot{q}_j \end{aligned} \quad (11)$$

Taking partial derivative of eq.(9) w.r.t  $q_i$  gives

$$\frac{\partial L}{\partial q_i} = \frac{1}{2} \sum_{j=1}^n \sum_{k=1}^n \frac{\partial D_{jk}}{\partial q_i} \dot{q}_k \dot{q}_j + \sum_{j=1}^n m_j {}^0g^T \frac{\partial {}^u r_{Li}}{\partial q_i} \quad (12)$$

Combining eqs.(11) and (12), the dynamic equation of motion for an n-link manipulator is obtained as

$$\left[ \sum_{j=1}^n D_{ij} \ddot{q}_j + \sum_{j=1}^n \sum_{k=1}^n \frac{\partial D_{ij}}{\partial q_k} \dot{q}_k \dot{q}_j \right] - \left[ \frac{1}{2} \sum_{j=1}^n \sum_{k=1}^n \frac{\partial D_{jk}}{\partial q_i} \dot{q}_k \dot{q}_j + \sum_{j=1}^n m_j {}^0g^T \frac{\partial {}^u r_{Li}}{\partial q_i} \right] = F_i \quad (13)$$

The effects of friction can also be modelled as a generalized force applied to the joints of the arm. Friction is a complex non-linear force that is difficult to model accurately, yet in many cases it can have a significant effect on robot arm dynamics. Thus the expression for the generalized force is

$$F_i = \tau_E - b_i(\dot{q}) \quad (14)$$

where  $\tau_E$  is joint torque vector generated by the elastic elements and actuators and it can be written as

$$\begin{aligned} \tau_E &= F_i + b_i(\dot{q}) \\ &= M(q)\ddot{q} + C(q, \dot{q})\dot{q} + G(q) + B(\dot{q}) \end{aligned} \quad (15)$$

where

$$M(q) = \sum_{j=1}^n D_{ij}(q) ; \text{ Inertia matrix}$$

$$C(q, \dot{q}) = \sum_{j=1}^n \sum_{k=1}^n \left( \frac{\partial D_{ij}}{\partial q_k} - \frac{1}{2} \frac{\partial D_{jk}}{\partial q_i} \right) \dot{q}_k \dot{q}_j ; \text{ Velocity coupling vector}$$

$$G(q) = \sum_{j=1}^n m_j {}^0g^T \frac{\partial {}^u r_{Li}}{\partial q_i} ; \text{ Gravitational force vector}$$

$$B(\dot{q}) = \text{Frictional force vector}$$

Thus eq.(15) shows the complete link side dynamics.

#### B4. Link Side Dynamic Model for 2 Link VSA Manipulator

Fig.2 depicts an ideal two link planar manipulator moving in the X-Y plane. Table 2 shows the notations used in fig.2

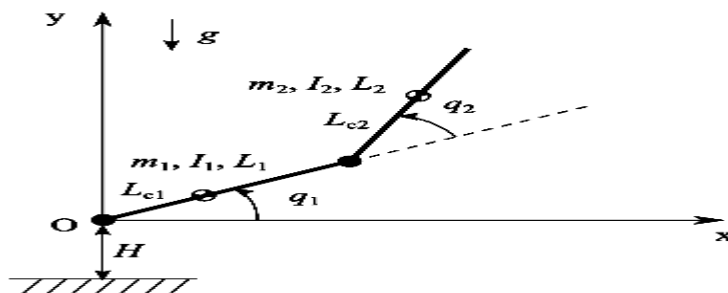


Fig 2: schematic drawing of a 2 link planar manipulator

Table 2: parameters of a 2 link manipulator

Notation	Description
$q_i$	Joint angle of joint i
$m_i$	Mass of link i
$I_i$	Moment of inertia of link i
$l_i$	Length of link i
$l_{ci}$	The distance between joint i and the center of mass of link i

The Lagrangian function of a 2 link manipulator is given by

$$L = K_1 + K_2 - V_1 - V_2$$

Where  $K_1 = \frac{1}{2}m_1\dot{q}_1^2 + \frac{1}{2}I_1\dot{q}_1^2$  : kinetic energy of link 1

$$K_2 = \frac{1}{2}m_2 \left( l_1\dot{q}_1^2 + l_{c2}^2(\dot{q}_1 + \dot{q}_2)^2 + 2l_1l_{c2}\dot{q}_1\cos q_2(\dot{q}_1 + \dot{q}_2) \right) + \frac{1}{2}I_2(\dot{q}_1 + \dot{q}_2)^2$$

kinetic energy of link 2

$$V_1 = m_1gl_{c1}\sin q_1$$
 : potential energy of link 1

$$V_2 = m_2g(l_1\sin q_1 + l_{c2}\sin(q_1 + q_2))$$
 : potential energy of link 2

Calculating L and substituting this into eq.(2) yields the equations of motions for the two link manipulator:

$$\tau_1 = [I_1 + I_2 + m_1l_{c1}^2 + m_2(l_1^2 + l_{c2}^2 + 2l_1l_{c2}\cos q_2)]\ddot{q}_1 + [m_2(l_{c2}^2 + l_1l_{c2}\cos q_2) + I_2]\ddot{q}_2 - m_2l_1l_{c2}\sin q_2(2\dot{q}_1\dot{q}_2 + \dot{q}_2^2) + m_1gl_{c1}\cos q_1 + m_2g(l_1\cos q_1 + l_{c2}\cos(q_1 + q_2)) \tag{16}$$

$$\tau_2 = [I_2 + m_2(l_{c2}^2 + l_1l_{c2}\cos q_2)]\ddot{q}_1 + (m_2l_{c2}^2 + I_2)\ddot{q}_2 + m_2l_1l_{c2}\sin q_2\dot{q}_1^2 + m_2gl_{c2}\cos(q_1 + q_2) \tag{17}$$

This can also be written as

$$\tau_1 = [M_{11}]\ddot{q}_1 + [M_{12}]\ddot{q}_2 + [C_{12}]\dot{q}_2^2 + 2[C_{11}]\dot{q}_1\dot{q}_2 + g_1 + b_1 \tag{18}$$

$$\tau_2 = [M_{21}]\ddot{q}_1 + [M_{22}]\ddot{q}_2 + [C_{21}]\dot{q}_1^2 + g_2 + b_2 \tag{19}$$

where

$$M_{11} = I_1 + I_2 + m_1l_{c1}^2 + m_2(l_1^2 + l_{c2}^2 + 2l_1l_{c2}\cos q_2)$$

$$M_{12} = M_{21} = m_2(l_{c2}^2 + l_1l_{c2}\cos q_2) + I_2$$

$$M_{22} = m_2l_{c2}^2 + I_2$$

$$C_{11} = C_{12} = -C_{21} = -m_2l_1l_{c2}\sin q_2$$

$$g_1 = m_1gl_{c1}\cos q_1 + m_2g(l_1\cos q_1 + l_{c2}\cos(q_1 + q_2))$$

$$g_2 = m_2gl_{c2}\cos(q_1 + q_2)$$

For a 2 link manipulator, the vector of elastic joint torques  $\tau_E$  can be represented as

$$\tau_E = \begin{bmatrix} \tau_1 \\ \tau_2 \end{bmatrix} = \rho \begin{bmatrix} T_1 - T_2 \\ T_3 - T_4 \end{bmatrix} \tag{20}$$

where  $T_i, i = 1, \dots, 4$  is the tension in each of the four tendons, and  $\rho$  is the joint radius, which is the same for both joints. As can be seen from Fig. 1, NEE 1 and NEE 2 are attached to the first joint, while NEE 3 and NEE 4 are attached to the second joint. NEEs are designed such that the tendon tensions are quadratic polynomial functions of the tendon displacements.

$$T_i = \alpha_i\delta_i^2 + \beta_i\delta_i + \gamma_i \tag{21}$$

where  $\alpha_i, \beta_i, \gamma_i$  are coefficients and  $\delta_i$  is the tendon displacement. The values of  $\delta_i$  can be calculated from joint geometry and system parameters as

$$\delta_1 = \delta_0 - \rho \left( q_1 + \frac{\pi}{2} \right) + \rho_2 \theta_1$$

$$\begin{aligned} \delta_2 &= \delta_0 + \rho \left( q_1 + \frac{\pi}{2} \right) - \rho_p \theta_2 \\ \delta_3 &= \delta_0 + \rho q_2 + \rho_p \theta_3 \\ \delta_4 &= \delta_0 - \rho q_2 - \rho_p \theta_4 \end{aligned} \quad (22)$$

where  $\delta_0$  and  $\rho_p$  being the initial displacement of NEEs and the radius of pulleys on motors (which is the same for all motors), respectively. Antagonistic configuration and nonlinear behaviour of the NEEs ensure variable compliance actuation.

### C. Motor Side Dynamics

Since the motor side dynamics is typically faster than the link-side dynamics, and since the stiffness modulation depends on the value of  $\theta$ , a separate control loop is usually employed for the position control of the motor side. The torque generated by each motor, which would be the "physical" input to the system, becomes a function of the motor variables  $\theta$  and  $\dot{\theta}$ , and of the reference angular positions, namely  $\theta_d \in R^{n_\theta}$ . Under the standard assumption of high gear reduction, and/or of high gain feedback position controllers, it is well known that the closed-loop dynamics of each motor can be represented by a linear second-order model, as

$$\ddot{\theta}_i + 2\varepsilon_i \dot{\theta}_i + k_i^2 \theta_i = k_i^2 \theta_{d,i}; i=1-4 \quad (23)$$

where  $\theta_i$  and  $\theta_{d,i}$  are the  $i$ -th components of  $\theta$  and  $\theta_d$ , respectively, while  $\varepsilon_i, k_i$  are constants associated to each motor dynamics. Their values can be related to the parameters of the motors and of their position controllers. Typically, position control is already implemented in the available commercial servomotors, and it is tuned such that the closed-loop dynamics is critically damped, i.e.,  $\varepsilon = k_i$ , in order to obtain the fastest possible response with no overshoot.

### D. State Space Model for an N-link VSA Robot

Various simulation software like Simulink/MATLAB, LabVIEW, etc are available for the simulation of a system described by differential equations or represented in state space equations. So first we need to express the obtained dynamic model of the VSA robotic system in form acceptable to simulation software. For this purpose here it is conveniently converted into its nonlinear state space form.

In order to obtain an overall nonlinear state-space model of the system, we define the state vector and the control input as

$$x = [q^T \dot{q}^T \theta^T \dot{\theta}^T]^T = [x_1^T x_2^T x_3^T x_4^T]^T \in R^{n_x}; n_x \triangleq 2n_q + 2n_{\theta} = n_d \in R^{n_d}$$

Then the over-all state space model of the system is

$$\dot{x} = f(x, u) = \begin{bmatrix} x_2 \\ -M^{-1}(x_1)[c(x_1, x_2)x_2 + Dx_2 + G(x_1) - \tau_E(x_1, x_2)] \\ x_4 \\ -Bx_4 - Kx_3 + Ku \end{bmatrix} \quad (24)$$

#### D1.State Space Model for a 2 Link VSA Robot Manipulator

For a two link manipulator, the joint angle and motor angle vectors are given by

$$q = [q_1 q_2]^T$$

$$\theta = [\theta_1 \theta_2 \theta_3 \theta_4]^T$$

Hence number of state variables,  $n_x$  will be obtained as  $2(2+4)=12$ .

i.e, we can define 12 state variables using these two coordinates and their derivatives as

$$x = [x_1 \ x_2 \ x_3 \ x_4 \ x_5 \ x_6 \ x_7 \ x_8 \ x_9 \ x_{10} \ x_{11} \ x_{12}]^T = [q_1 \ q_2 \ \dot{q}_1 \ \dot{q}_2 \ \theta_1 \ \theta_2 \ \dot{\theta}_1 \ \dot{\theta}_2 \ \ddot{q}_1 \ \ddot{q}_2 \ \ddot{\theta}_1 \ \ddot{\theta}_2]^T$$

## V. CONTROLLER DESIGN

Open loop response of the VSA robot manipulator for a unit step input is shown in fig.3. It contains initial vibrations and settles at a steady state value of 1.9, which obviously requires to be controlled by a proper control signal to meet the specifications required.

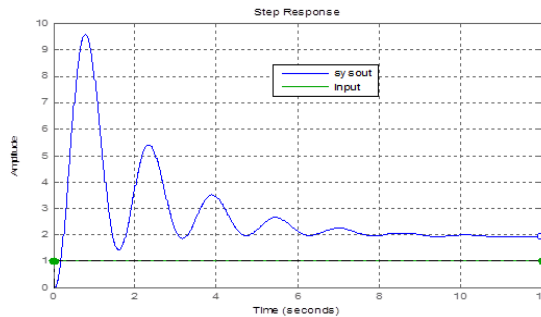


Fig.3. open loop response of the system

### A .PD and PID Controllers

Proportional action provides an instantaneous response to the control error. This is useful for improving the response of a stable system but cannot control an unstable system by itself. Additionally, the gain is the same for all frequencies leaving the system with a nonzero steady-state error. Derivative action acts on the derivative or rate of change of the control error. This provides a fast response, as opposed to the integral action, but cannot accommodate constant errors (i.e. the derivative of a constant, nonzero error is 0). Proportional-Derivative or PD control combines proportional control and derivative control in parallel.

Properly designed PD controllers can affect the performance of a control system in the following ways:

- \*Improve damping and reduce maximum overshoot
- \*Reduce rise and settling time

PID controller has all the necessary dynamics: fast reaction on change of the controller input (D mode), increase in control signal to lead error towards zero (I mode) and suitable action inside control error area to eliminate oscillations (P mode). PID controller is used when dealing with higher order capacitive processes) when their dynamic is not similar to the dynamics of an integrator (like in many thermal processes). PID controller is often used industry, but also in the control of mobile objects) when stability and precise reference following are required.

## VI. SIMULATION RESULTS AND DISCUSSIONS

Simulation result of the system when placed a PD controller and PID controller is shown in Fig.4. Trajectory followed by link 1 is shown in Fig.4(a) and that followed by link 2 is shown in Fig.4(b). It is clear from the figures that response is very much oscillatory for PD controller and it gives a steady state value of 0.88 which is not at all acceptable since the trajectory given to track is a unit step. By adding an integral gain, a PID controller has designed and it has somewhat modified the robotic system response in such a way that amplitude settles at unity and only a small amount of initial vibration exists.



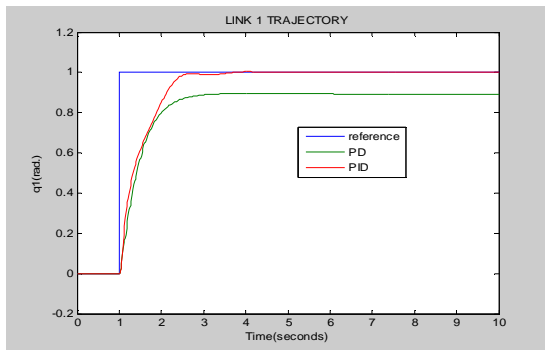


Fig.4(a)

Fig. 4(a): Response of the system using PD and PID for Link 1

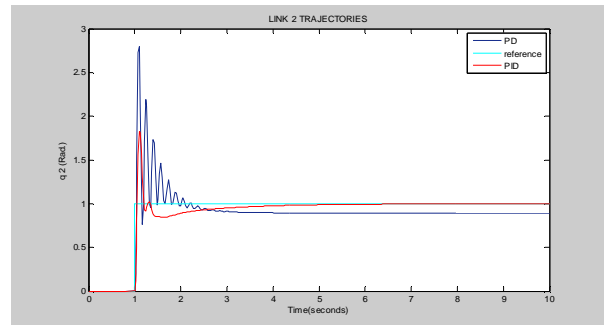


Fig.4(b)

Fig. 4(b): Response of the system using PD and PID for Link 2

## VI. CONCLUSIONS

The system of variable stiffness actuated robot modelled using Lagrange-Euler formulation method and the obtained model validated using MATLAB simulation software for a reference signal of unit step signal. Linear control strategies like PD and PID are simulated in the same software by manual tuning for checking whether the system model faithfully tracks the assigned input path. Simulation results have shown that PID controller gives faster settling times, less vibration and less overshoot for the angular position response as compared to PD controller.

## REFERENCES

- [1] B. Siciliano and O. Khatib, Eds., *Springer Handbook of Robotics*. New York, NY, USA: Springer-Verlag, 2008.
- [2] G. Hirzinger, J. Bals, M. Otter, and J. Stelter, "The DLR- KUKA success story: Robotics research improves industrial robots," *IEEE Robot. Autom. Mag.*, vol. 12, no. 3, pp.16\_23, Sep. 2005.
- [3] A. Albu-Schaffer *et al.*, "Soft robotics," *IEEE Robot. Autom. Mag.*, vol. 15, no. 3, pp. 20\_30, Sep. 2008.
- [4] C. English and D. Russell, "Implementation of variable joint stiffness through antagonistic actuation using rolamite springs," *Mech. Mach. Theory*, vol. 34, no. 1, pp. 27\_40, 1999.
- [5] K. Koganezawa, Y. Watanabe, and N. Shimizu, "Antagonistic muscle-like actuator and its application to multi-d.o.f. forearm prosthesis," *Adv. Robot.*, vol. 12, nos. 7\_8, pp. 771\_789, 1997.
- [6] S. Wolf and G. Hirzinger, "A new variable stiffness design: Matching requirements of the next robot generation," in *Proc. Int. Conf. Robot. Autom.*, May 2008, pp. 1741\_1746.
- [7] S. Wolf, O. Eiberger, and G. Hirzinger, "The DLR FSJ: Energy based design of a variable stiffness joint," in *Proc. IEEE Int. Conf. Robot. Autom.*, May 2011, pp. 5082\_5089.
- [8] D. J. Braun, F. Petit, F. Huber, S. Haddadin, P. van der Smagt, A. Albu-Schaffer, and S. Vijayakumar, "Robots driven by compliant actuators: Optimal control under actuation constraints," *IEEE Trans. Robot.*, vol. 2, no. 5, pp. 1085-1101, Oct. 2013.
- [9] B. Vanderborght, N. Tsagarakis, R. VanHam, I. Thorson, and D. Caldwell, "MACCEPA 2.0: Compliant actuator used for energy efficient hopping robot chobino 1D," *Auton. Robots*, vol. 31, no. 1, pp. 55-65, 2011.
- [10] S. A. Migliore, E. A. Brown, and S. P. DeWeerth, "Biologically inspired joint stiffness control," in *Proc. of the IEEE/RSJ International Conference on Intelligent Robots and Systems*, 2005, pp. 4519-4524.
- [11] A. D. Luca and P. Lucibello, "A general algorithm for dynamic feedback linearization of robots with elastic joints," in *Proc. IEEE Int. Conf. on Robotics and Automation*, 1998.
- [12] G. Tonietti, R. Schiavi, and A. Bicchi. "Design and control of a variable stiffness actuator for safe and fast physical human/robot interaction." *Int. Conf. on Rob. and Aut.*, pages 526-531, 2005.
- [13] G. Palli, C. Melchiorri, and A. De Luca. On the feedback linearization of robots with variable joint stiffness. *Int. Conf. on Rob. and Aut.*, pages 1753-1759, 2008.
- [14] A. De Luca, F. Flacco, A. Bicchi, and R. Schiavi. "Nonlinear decoupled motion-stiffness control and collision detection/reaction for the vsai variable stiffness device," *Int. Conf. on Int. Rob. and Sys.*, pages 5487-5494, 2009.
- [15] J. S. Shamma and M. Athans. Gain scheduling: "Potential hazards and possible remedies," *IEEE Control Systems Magazine*, pages 101-107, 1992.